

Synthesis and Characteristics of Microencapsulated Myristic Acid with TiO₂ as Composite Thermal Energy Storage Materials

Zhaohe WANG, Yanghua CHEN*

College of Mechatronics Engineering, Nanchang University, Nanchang 330031, China

crossref <http://dx.doi.org/10.5755/j02.ms.25098>

Received 16 January 2020; accepted 25 March 2020

To solve the issues of flowing and leaking of myristic acid (MA) as phase change energy storage material in practical application, a novel microencapsulated composite phase change energy storage material was prepared by sol-gel method using myristic acid (MA) as core material and titanium dioxide (TiO₂) as shell material. The chemical structure, crystal structure, micromorphology, phase change characteristics and thermal stability of phase change microencapsulated energy storage materials were characterized by using Fourier transform infrared spectrometer (FT-IR), X-ray diffraction analyzer (XRD), field emission scanning electron microscope (FE-SEM), differential scanning calorimetry (DSC), thermogravimetric analyzer (TGA). The consequents illustrated that the ideal sample melted at 54.97 °C with the latent heat of 55.76 J/g and solidified at 49.85 °C with the latent heat of 54.55 J/g. In general, the prepared microencapsulated phase change materials possessed good thermal properties and thermal stabilities. It is predicted that the shape-stabilized MA/TiO₂ composites have great potential for thermal energy storage.

Keywords: myristic acid, sol-gel method, phase change microcapsule, composite.

1. INTRODUCTION

Phase change materials (PCMs) can accomplish storage and release of energy, thereby solving the current issue of mismatching demand and supply of thermal energy and alleviating many contradictions between energy and environmental pollution [1]. As an ideal phase change material, organic phase transition material can absorb or release much heat from the environment during its melting or solidification process while keeping the temperature unchanged [2]. However, the organic phase change materials are fluid and amorphous after melting, which will lead to the leakage problem during working and hinder the application of organic phase change materials in practice.

Phase change microcapsule technology, which encapsulates organic phase change materials in a solid shell to make organic materials microencapsulated, can prevent leakage of organic phase transition materials [3]. Microencapsulation of phase transition materials can increase the heat conduction area of phase transition materials, control the volume change of the phase transition process and also overcome the weakness of leakage of phase change materials [2,4]. Microencapsulation of materials can maintain the heat storage performance of phase change materials and also can be widely used in building energy-saving system [5,6], air conditioning systems [7,8], solar energy and military camouflage [9,10], thermally regulated textile materials [11,12] and other practical areas of energy utilization [13]. Cao et al. [14] synthesized palmitic acid microcapsules with TiO₂ shell by sol-gel method. The results showed that the prepared microcapsules were non-flammable, non-toxic, good thermal properties and large potential for energy. Chen et al. [15] prepared a novel phase transition microencapsulated material with lauric acid as the

core material and titanium dioxide as the shell material by the sol-gel method. The results illustrated that the composite material has good thermal stability during the working temperature range. Microencapsulated composite materials can be applied to solar storage electronics. Chen et al. [16] prepared a microencapsulated material by sol-gel method using stearic acid as the core material and SiO₂ as the shell. Zhou et al. [17] used titanium dioxide as the shell material and paraffin as the core material to make microcapsules. The outcomes stated that they have good thermal properties and thermal stability.

In this paper, microencapsulated myristic acid composite phase transition energy storage material using TiO₂ as shell material was synthesized by sol-gel method. As an organic nuclear material, myristic acid has the characteristics of small volume change, no phase separation, small undercooling, appropriate phase transformation temperature and higher latent heat values. As a shell material, TiO₂ has the advantages of thermal stability, chemical stability, fire resistance, high thermal conductivity, non-toxic and no-corrosion [18–22]. To our knowledge, there are few reports about myristic acid/titanium dioxide microcapsule materials. The main content of this study is to synthesize microencapsulated composite materials with titanium dioxide as shell material. The samples were characterized by FT-IR, XRD, FE-SEM, DSC and TGA. The prepared microcapsule composites will have a broad application in the field of energy storage.

2. EXPERIMENT

2.1. Experimental materials and instruments

Myristic acid (C₁₄H₂₈O₂, purity ≥ 99 %, AR) was used as the phase transition material. As the precursor, tetrabutyl

* Corresponding author. Tel.: +86-13970944938.
E-mail address: chyhix@163.com (Y. Chen)

titanate ($C_{16}H_{36}O_4Ti$, AR) can generate titanium dioxide by hydrolysis and condensation reaction. Sodium dodecyl sulfate ($C_{12}H_{25}SO_4Na$, AR) was used as an emulsifier. The above three experimental materials were got from Aladdin Chemical Reagent CO., Ltd. Anhydrous alcohol (C_2H_5OH , AR) and deionized water were used as solvents. Hydrochloric acid (HCl, concentration 36 %–38 %) was used as a catalyst and stabilizer. They were purchased from Xilong Chemical Reagent Company.

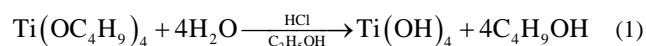
Type FA1004N electronic balance was obtained from Wante Electronics Shanghai Co., Ltd., JP-008 type ultrasonic cleaning machine was received from Shenzhen Energy-saving Cleaning Equipment Co., Ltd. DZF-6210 vacuum drying box and digital display constant temperature magnetic stirring water bath pot were purchased from Shanghai Jinghong Experimental Equipment Co., Ltd. and Changzhou Langyue Instrument Manufacturing Co., Ltd. respectively.

Nicolet 5700 Fourier Transform Infrared Spectrometer (FT-IR) was produced in Thermoelectric Nicoll Corporation, D8 ADVANCE X-Ray Diffraction (XRD) was got from Bruker, Germany, JSM 6701F Field Emission Scanning Electron Microscope was selected from Japan JEOL Company, DSC 8500 Differential Scanning Calorimeter (DSC) was produced in American PE Company and TGA 4000 Thermogravimetric Analyzer (TGA) was obtained from American PE Company.

2.2. Preparation of the microencapsulated MA with TiO_2 shell

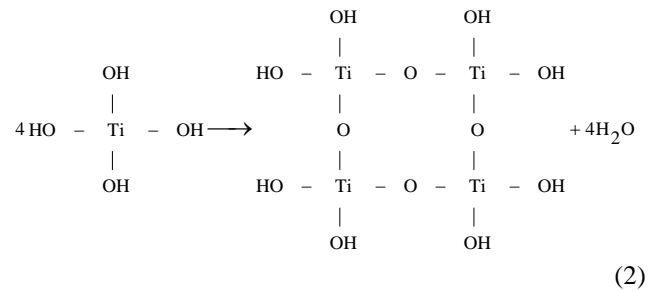
The myristic acid and sodium dodecyl sulfate in different mass ratio (listed in Table 1.) were added to the beaker containing deionized water. Next, placed the beaker in a thermostatic magnetic stirring water bath, kept the heating temperature of the water bath at 70 °C, the stirring speed at 500 rpm/min, and maintained this temperature and stirring speed for 50 minutes until the myristic acid is evenly distributed in the O/W microemulsion. Then, hydrochloric acid dropwise was added to beaker to regulate the pH of the microemulsion to 2–3.

The absolute ethanol and tetrabutyl titanate (TBOT) were mixed together in a beaker to form liquor at room temperature in accordance with the ratio listed in Table 1. Then, it was added dropwise to the synthesized myristic acid microemulsion. In the meantime, the temperature and mixing speed of the thermostatic magnetic mixing water bath were dominated at 70 °C and 500 rpm/min for 1 hour. In this process, TBOT first hydrolyses with water to form titanate monomer (Eq. 1). Eq. 1 depicts hydrolytic reaction of TBOT.



Subsequently, these monomers undergo a

polymerization reaction, forming bonds with each other, and finally the oligomers gradually polymerize and deposit on the surface of the myristic acid microemulsion to form a dioxin shell. The specific condensation reaction of TBOT:



Principle of titanium dioxide formation:

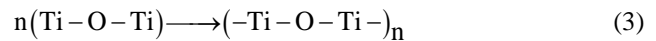


Fig. 3. Principle of titanium dioxide formation

Finally, the mixture in the beaker was filtered and washed with water, and then placed in a vacuum drying oven at 45 °C for 24 hours. At last, there were three kinds of microcapsules were prepared, which named as MPCM1, MPCM2 and MPCM3.

2.3. Characterizations of the prepared microencapsulated MA with TiO_2 shell

The infrared spectrum of myristic acid, titanium dioxide and three kinds of microencapsulated composites were measured by FT-IR. The KBr compression method was used in the sample preparation. The measurement frequency range was from 4000 cm^{-1} to 400 cm^{-1} , and the accuracy was 0.09 cm^{-1} . The angular position and intensity of sample diffraction were performed and recorded using XRD to analyze the crystal structure inside the microcapsule phase change material. The scanning speed was 5° (2θ)/min, the working voltage was 40 kV, and the working current was 40 mA. The morphology of TiO_2 and three microencapsulated composites were observed by using FE-SEM. DSC was used to determine the thermal performance parameters such as phase change temperature and phase change latent heat of myristic acid and three kinds of microcapsules. The heating and cooling rates were both 5 °C/min. The measurement process was under a nitrogen protection environment with a purging rate of 20 ml/min. And the range is from 10 °C to 90 °C [23]. TGA was used to investigate the thermal stability of myristic acid and three kinds of microcapsules. The measurement process was under in a nitrogen-protected environment, and the temperature measurement range was from room temperature to 700 °C [24].

Table 1. The components of the MA emulsion and solution of the TBOT

Samples	Myristic acid emulsion			Solution of the tetrabutyl titanate	
	Myristic acid, g	Deionized water, ml	SDS, g	Tetrabutyl titanate, g	Anhydrous alcohol, g
MPCM1	4	60	0.7	7	16
MPCM2	3	60	0.5	7	16
MPCM3	3	60	0.5	7	20

3. RESULTS AND DISCUSSION

3.1. FT-IR analysis of the microencapsulated MA with TiO₂ shell

FT-IR analysis of myristic acid, titanium dioxide, MPCM1, MPCM2 and MPCM3 microcapsules are presented in Fig. 4. As seen in Fig. 4 a, the weaker absorption peak at 2957.16 cm⁻¹ represented the asymmetric stretching vibration of the -CH₃ group in the myristic acid molecule; two strong absorptions at 2918.40 cm⁻¹ and 2848.37 cm⁻¹ The peak meant the asymmetric and symmetrical stretching vibration of the -CH₂ group [25], the strong absorption peak at 1701.28 cm⁻¹ indicated the stretching vibration of the C=O group.

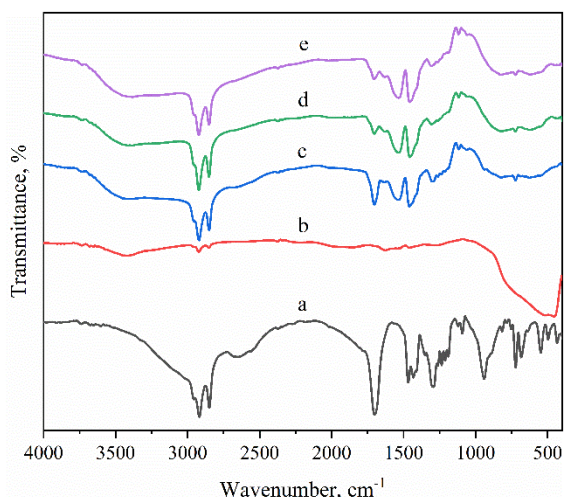


Fig. 4. FT-IR spectrum of: a–MA; b–TiO₂; c–MPCM1; d–MPCM2; e–MPCM3

A series of absorption peaks appearing near 1468.21 cm⁻¹, 1236.10 and 722.12 cm⁻¹ were caused by the bending vibration of the -CH₃ group and the -CH₂ group. The absorption peaks at 1292.00 cm⁻¹ and 940.93 cm⁻¹ represented rocking vibrations of -OH groups out of plane, while the absorption peaks at 722.12 cm⁻¹ indicated rocking vibrations of -CH₂ groups in plane. It could be seen in Fig. 4 b that the stretching vibration and bending vibration of -OH in H₂O were at 3421.05 cm⁻¹ and 1628.49 cm⁻¹. In Fig. 4, there was no absorption peak of titanium dioxide, which is because the characteristic peak of titanium dioxide was in the far-infrared region [26]. As seen in Fig. 4 c to Fig. 4 e, the infrared spectra of the three MPCMs contained all characteristic peaks of myristic acid and the absorption bands of the titanium dioxide infrared spectra. In addition, all the characteristic peaks had not shifted. Therefore, there was no chemical reaction between myristic acid and titanium dioxide, and the microcapsules prepared were only physical combination between the two.

3.2. XRD analysis of the microencapsulated myristic acid with TiO₂ shell

The XRD patterns of myristic acid, titanium dioxide, MPCM1, MPCM2, and MPCM3 microcapsules are shown in Fig. 5. They were represented by curves a, b, c, d and e, respectively. In Fig. 5 a, there were significant diffraction peaks at 21.8° and 24.6°, which was because myristic acid had a regular crystal structure. In Fig. 5 b, the diffraction

peak of titanium dioxide relative to myristic acid was relatively flat, which indicated that it was an amorphous material. As shown in Fig. 5 c to Fig. 5 e, the XRD patterns of the three MPCMs included all characteristic peaks of myristic acid without additional characteristic peaks appeared. The characteristic peaks of the microencapsulated composites were compared to the characteristics of myristic acid and titanium dioxide. The peak did not shift, which indicated that the crystal structure of the two did not change after microencapsulated myristic acid with titanium dioxide shell.

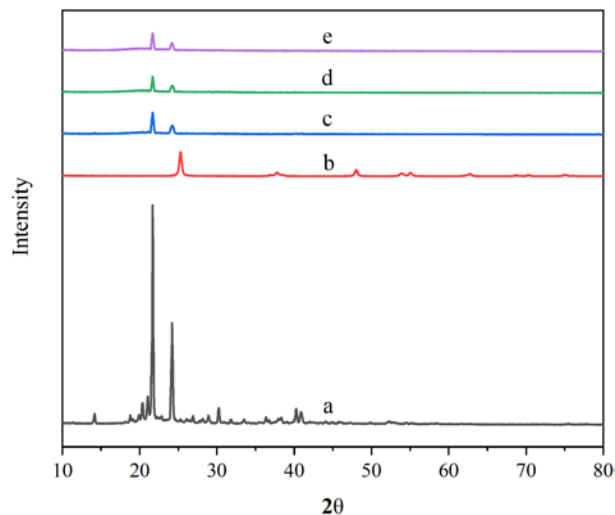


Fig. 5. XRD patterns of: a–MA; b–TiO₂; c–MPCM1; d–MPCM2; e–MPCM3

3.3. FE-SEM analysis of the microencapsulated MA with TiO₂ shell

The surface morphology and microstructure of microencapsulated myristic acid with titanium dioxide shell were observed by field emission scanning electron microscopy. Fig. 6. represents SEM photographs of titanium dioxide and three MPCMs. It could be seen in the pictures that the size of phase change microcapsules was about nanometers. Titanium dioxide coated myristic acid is a physical effect, forming microencapsulated myristic acid with titanium dioxide shell microcapsules, which played a role in preventing myristic acid from leaking. It could be known that the prepared microcapsules were well encapsulated into micro-nano-level ellipsoidal particles or flocculent particle clusters by the TiO₂ shell. Some similar results had been obtained in previous studies on microcapsules with TiO₂ shell [14, 15].

3.4. Thermal properties analysis of the microencapsulated MA with TiO₂ shell

Fig. 7 and Fig. 8 represented the DSC curves of the melting and solidifying processes of myristic acid, MPCM1, MPCM2 and MPCM3, respectively. Some specific parameters of thermodynamic properties such as phase transition temperature and phase transition latent heat during the melting and solidification processes of myristic acid and MPCM microcapsules are presented in Table 2. As seen in Table 2, the melting temperatures of myristic acid, MPCM1, MPCM2 and MPCM3 were 57.65 °C, 54.97 °C, 54.63 °C, and 54.76 °C, respectively.

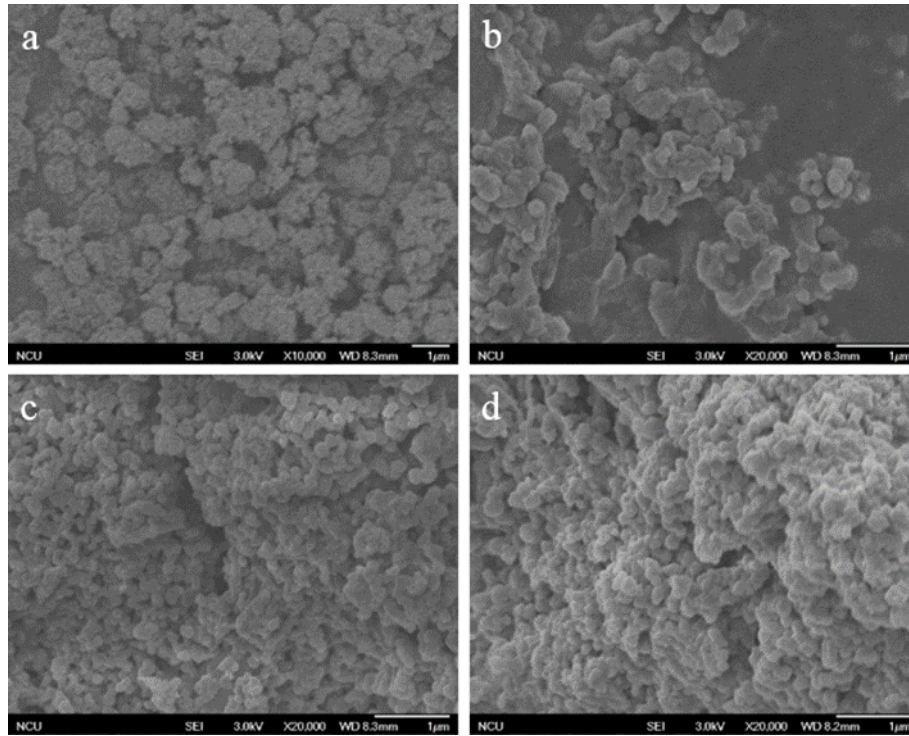


Fig. 6. FE-SEM pictures of: a – TiO₂(10k×); b – MPCM1(20k×); c – MPCM2(20k×); d – MPCM3(20k×)

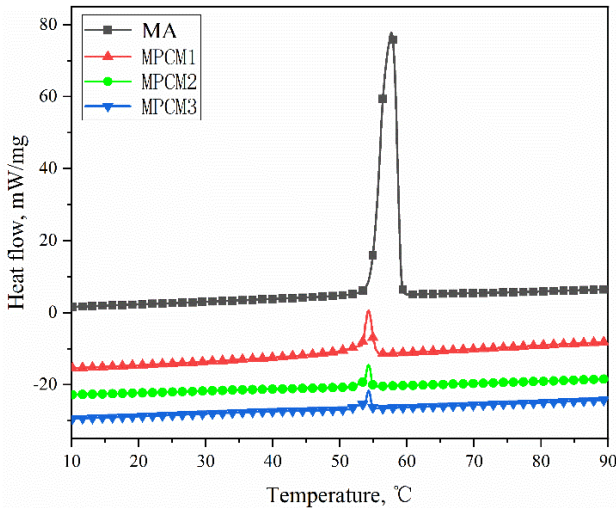


Fig. 7. The melting DSC curves of the MA, MPCM1, MPCM2 and MPCM3

The solidifying temperatures were 51.26 °C, 49.85 °C, 49.40 °C and 47.22 °C, respectively. The difference between the melting and solidifying temperatures of myristic acid was 6.39 °C, while the differences between the melting and solidifying temperatures of MPCM1, MPCM2 and MPCM3 were 5.12 °C, 5.23 °C and 5.54 °C, respectively. This demonstrated that the titanium dioxide shell promoted the nucleation of myristic acid during the solidification process and reduced the subcooling of the microencapsulated composites.

The mass fraction of myristic acid in the microcapsules can be calculated by equation [27]:

$$\omega = \frac{\Delta H_{MPCM}}{\Delta H_{MA}} \times 100\% , \quad (4)$$

where ω represents the mass fraction of myristic acid contained in the microencapsulated composites, ΔH_{MA} represents the latent melting heat of myristic acid (J/g) and ΔH_{MPCM} means the melting latent heat of microencapsulated phase change material (J/g).

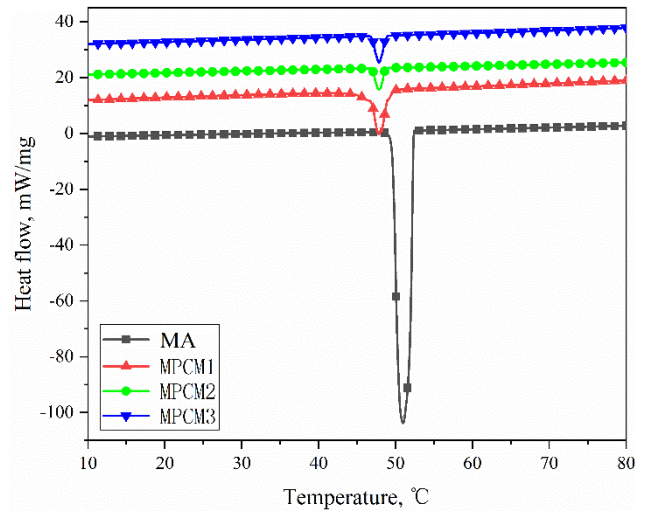


Fig. 8. The solidifying DSC curves of the MA, MPCM1, MPCM2 and MPCM3

The mass fractions of myristic acid in the microcapsules MPCM1, MPCM2 and MPCM3 were calculated to be 28.03 %, 16.18 % and 18.36 %, respectively. According to only myristic acid as the core material played a role of absorbing and releasing energy in the microencapsulated materials. Therefore, the higher the mass fraction of myristic acid existed in the composite phase transition material, the higher the storing energy and the stronger the ability of the microencapsulated composite materials.

As presented in Table 2, the enthalpy of transformation of MPCM1 was higher than that of MPCM2 and MPCM3. For MPCM2 and MPCM3, the difference in the mass fractions of myristic acid contained in the microcapsules was caused by the difference in the concentration of anhydrous ethanol in the TBOT solution during the preparing process, which indicated that the concentration of anhydrous ethanol would affect the mass fraction of myristic acid contained in the microcapsules [27]. This is because anhydrous ethanol could dilute the TBOT solution and prevent the hydrolysis rate of TBOT from being too fast, which was beneficial to the production of the TiO₂ shell [14]. In summary, MPCM1 was selected as the satisfactory sample. The microcapsule melted at 54.97 °C with the latent heat of 55.76 J/g and solidified at 49.85 °C with the latent heat of 54.55 J/g.

Some data about the microencapsulated MA with TiO₂ shell and microcapsules in other literatures were given in Table 3. It demonstrated that the synthesized microencapsulated MA with TiO₂ had suitable phase change temperature and higher melting and solidifying latent heat comparing with other microcapsule materials. It indicated that it possesses bright application prospects in energy storage fields such as heat recovery systems, solar heating systems and building energy-saving systems.

3.5. Thermal stability analysis of the microencapsulated MA with TiO₂ shell

The TGA curves of myristic acid, MPCM1, MPCM2 and MPCM3 are given in Fig. 9. The onset temperature (T_{onset}), the corresponding temperature (T_{peak}) and the residual mass percentage (700 °C) of thermal decomposition of myristic acid and three MPCM samples were listed in Table 4. As shown in Fig. 9, the TGA curve of myristic acid was very steep and its degradation process was a one-step degradation process, which was because its molecule was a chain alkane structure and the decomposition temperature was lower [14].

Comparing with pure myristic acid, the TGA curve of the microcapsules were gentler. During the degradation process, the fastest weight loss temperatures of the three MPCM microcapsules were 395 °C, 387 °C and 382 °C, respectively, which were higher than the thermal decomposition temperature 277 °C of myristic acid. That signified that the titanium dioxide shell could inhibit the

degradation of myristic acid.

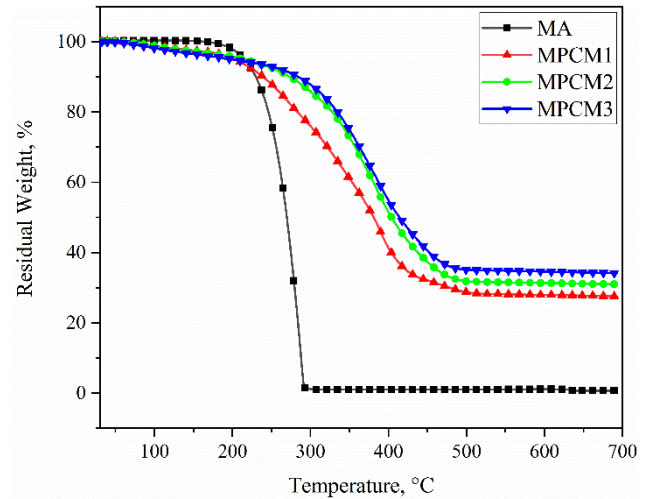


Fig. 9. TGA curves of the MA, MPCM1, MPCM2 and MPCM3

Table 4. TGA values of the MA, MPCM1, MPCM2 and MPCM3

Samples	T_{onset} , °C	T_{peak} , °C	Residual mass percentage, % 700 °C
Myristic acid	165	277	1.01 (310 °C)
MPCM1	76	395	26.83
MPCM2	68	387	29.98
MPCM3	63	382	33.15

The residual amount of myristic acid in the microcapsules was close to zero at 310 °C, while the residual amounts of MPCM1, MPCM2 and MPCM3 at this temperature were 73.36 %, 83.91 %, and 85.97 %, respectively. Because titanium dioxide as a protective shell formed a physical protective layer outside the myristic acid, which could prevent the escape of the flammable gas generated during the exudation of molten myristic acid and thermal decomposition [26]. During the working temperature range (30–80 °C) of microencapsulated myristic acid with titanium dioxide shell, their mass losses were less than 1.2 %. These results demonstrated that it could effectively improve their thermal stability and also has a positive effect on reducing its flammability by encapsulating myristic acid in a titanium dioxide shell. It can be applied to many fields such as solar energy storage system and building energy-saving system.

Table 2. DSC values of the MA, MPCM1, MPCM2 and MPCM3

Samples	Melting process		Solidifying process		Mass fraction of myristic acid, %
	Melting point, °C	Melting enthalpy, J/g	Solidifying point, °C	Solidifying enthalpy, J/g	
Myristic acid	57.65	198.93	51.26	196.70	100
MPCM1	54.97	55.76	49.85	54.55	28.03
MPCM2	54.63	32.18	49.40	30.87	16.18
MPCM3	54.76	36.52	49.22	33.71	18.36

Table 3. Comparison of the microcapsules between this study and other literatures

Materials	Types	Melting temperature, °C	Melting enthalpy, J/g	Solidifying temperature, °C	Solidifying enthalpy, J/g	References
Lauric acid/TiO ₂	MPCM	44.67	38.94	43.36	37.28	[15]
Stearic acid/TiO ₂	MPCM	53.84	47.82	53.31	45.60	[26]
Myristic acid/bentonite	MPCM	53.20	54.50	49.40	56.50	[28]
Palmitic acid/TiO ₂	MPCM	60.70	33.10	51.80	16.20	[14]
Myristic acid/TiO ₂	MPCM	54.97	55.76	49.85	54.55	Present study

4. CONCLUSIONS

In this study, the preparation and thermal characteristics of microencapsulated myristic acid with TiO₂ composites were presented. In microencapsulated phase change materials, myristic acid acted as phase transition material to absorb and release energy. While TiO₂ as the shell, which acted as a supporting and protecting material, effectively prevented the myristic acid from leakage during the phase transition process and enhanced the thermal stability of the microcapsule phase transition materials. FT-IR analysis revealed that there was only the result of physical adsorption between the compound process of myristic acid and TiO₂ without chemical reaction occurred. XRD analysis showed that the crystal structure of myristic acid and TiO₂ had no change after the phase change microcapsules were formed. FE-SEM analysis indicated that the TiO₂ shell was well wrapped with myristic acid and formed micro-nano-sized particle size ellipsoidal phase change microcapsule materials. Based on the results of DSC, TGA and FE-SEM, a kind of satisfactory sample was found. The ideal sample melted at 54.97 °C with the latent heat of 55.76 J/g and solidified at 49.85 °C with the latent heat of 54.55 J/g. The experimental measurement results signified that the microencapsulated myristic acid with TiO₂ shell composites obtained good thermal stability and higher latent heat comparing with some similar microcapsules. It is deduced that the synthesized microencapsulated myristic acid with TiO₂ shell possesses great potential and prospect in the fields of energy storage and utilization.

Acknowledgments

This work was supported by the Science and Technology Supporting Program of Jiangxi Province, China (No. 20112BBE50031). The authors also wish to thank the reviewers and editors for kindly giving revising suggestions.

REFERENCES

1. **Chai, L.X., Wang, X.D., Wu, D.Z.** Development of Bifunctional Microencapsulated Phase Change Materials with Crystalline Titanium Dioxide Shell for Latent-heat Storage and Photocatalytic Effectiveness *Applied Energy* 138 2015: pp. 661–674.
<http://dx.doi.org/10.1016/j.apenergy.2014.11.006>
2. **Zhao, C.Y., Zhang, G.H.** Review on Microencapsulated Phase Change Materials (MEPCMs): Fabrication, Characterization and Applications *Renewable & Sustainable Energy Reviews* 15 (8) 2011: pp. 3813–3832.
<http://dx.doi.org/10.1016/j.rser.2011.07.019>
3. **Cho, J.S., Kwon, A., Cho, C.G.** Microencapsulation of Octadecane as Phase Change Material by Interfacial Polymerization in an Emulsion System *Colloid and Polymer Science* 280 2002: pp. 260–266.
<http://dx.doi.org/10.1007/s00396-001-0603-x>
4. **Memon, S.A., Lo, T.Y., Cui, H.Z., Barbhuiya, S.** Preparation, Characterization and Thermal Properties of Dodecanol/cement as Novel Form-stable Composite Phase Change Material *Energy and Buildings* 66 2013: pp. 697–705.
<https://doi.org/10.1016/j.enbuild.2013.07.083>
5. **Wang, Y., Xia, T.D., Zheng, H., Feng, H.X.** Stearic Acid/silica Fume Composite as Form-stable Phase Change Material for Thermal Energy Storage *Energy and Buildings* 43 2011: pp. 2365–2370.
<https://doi.org/10.1016/j.enbuild.2011.05.019>
6. **Li, H., Liu, X., Fang, G.Y.** Preparation and Characteristics of N-nonadecane/cement Composite as Thermal Energy Storage Materials in Buildings *Energy and Buildings* 42 2010: pp. 1661–1665.
<https://doi.org/10.1016/j.enbuild.2010.04.009>
7. **Diaconu, B.M., Varga, S., Oliveira, A.C.** Experimental Assessment of Heat Storage Properties and Heat Transfer Characteristics of a Phase Change Material Slurry for Air Conditioning Applications *Applied Energy* 87 2010: pp. 620–628.
<https://doi.org/10.1016/j.apenergy.2009.05.002>
8. **He, B., Setterwall, F.** Technical Grade Paraffin Waxes as Phase Change Materials for Cool Thermal Storage and Cool Storage Systems Capital Cost Estimation *Energy Conversion and Management* 43 2002: pp. 1709–1723.
[https://doi.org/10.1016/S0196-8904\(01\)00005-X](https://doi.org/10.1016/S0196-8904(01)00005-X)
9. **Zalba, B., Marin, J.M., Cabeza, L.F., Mehling, H.** Review on Thermal Energy Storage with Phase Change: Materials, Heat Transfer Analysis and Applications *Applied Thermal Engineering* 23 (3) 2003: pp. 251–283.
[https://doi.org/10.1016/S1359-4311\(02\)00192-8](https://doi.org/10.1016/S1359-4311(02)00192-8)
10. **Saman, W., Bruno, F., Halawa, E.** Thermal Performance of PCM Thermal Storage Unit for a Roof Integrated Solar Heating System *Solar Energy* 78(2) 2005: pp. 341–349.
<https://doi.org/10.1016/j.solener.2004.08.017>
11. **Sarier, N., Onder, E.** The Manufacture of Microencapsulated Phase Change Materials Suitable for the Design of Thermally Enhanced Fabrics *Thermochimica Acta* 452 (2) 2007: pp. 149–160.
<https://doi.org/10.1016/j.tca.2006.08.002>
12. **Shin, Y., Yoo, D.I., Son, K.** Development of Thermoregulating Textile Materials with Microencapsulated Phase Change Materials (PCM). IV. Performance Properties and Hand of Fabrics Treated with PCM Microcapsules *Journal of Applied Polymer Science* 97 (3) 2005: pp. 2005–2010.
<https://doi.org/10.1002/app.21846>
13. **Sharma, S.D., Sagara, K.** Latent Heat Storage Materials and Systems: a Review *International Journal of Green Energy* 2 (1) 2005: pp. 1–56.
<https://doi.org/10.1081/GE-200051299>
14. **Cao, L., Tang, F., Fang, G.Y.** Preparation and Characteristics of Microencapsulated Palmitic Acid with TiO₂ Shell as Shape-stabilized Thermal Energy Storage Materials *Solar Energy Materials & Solar Cells* 123 2014: pp. 183–188.
<https://doi.org/10.1016/j.solmat.2014.01.023>
15. **Chen, Y.H., Liu, Y., Wang, Z.H.** Preparation and Characteristics of Microencapsulated Lauric Acid as Composite Thermal Energy Storage Materials *Materials Science (Medžiagotyra)* 26 (1) 2020: pp. 88–93.
<http://dx.doi.org/10.5755/j01.ms.26.1.21303>
16. **Chen, Z., Cao, L., Shan, F., Fang, G.Y.** Preparation and Characteristics of Microencapsulated Stearic Acid as Composite Thermal Energy Storage Material in Buildings *Energy and Buildings* 62 2013: pp. 469–474.
<https://doi.org/10.1016/j.enbuild.2013.03.025>

17. **Zhou, L.X., Wang, B.M., Tian, Y.T., Liu, Y., Liu, L., Lu, L.M., Tang, J.W.** Preparation and Characterization of Titanium Dioxide-Coated Paraffin Phase Change Microcapsules *Modern Chemical Industry* 39 (3) 2019: pp. 82–86.
18. **Li, W., Song, G., Li, S., Yao, Y.W., Tang, G.Y.** Preparation and Characterization of Novel MicroPCMs (microencapsulated phase change materials) with Hybrid Shells Via the Polymerization of Two Alkoxy Silanes *Energy* 70 2014: pp. 298–306.
<https://doi.org/10.1016/j.energy.2014.03.125>
19. **Yuan, Y.P., Zhang, N., Tao, W.Q., Cao, X.L., He, Y.L.** Fatty Acids as Phase Change Materials: A Review *Renewable & Sustainable Energy Reviews* 29 2014: pp. 482–498.
<https://doi.org/10.1016/j.rser.2013.08.107>
20. **Sari, A., Karaipekli, A.** Preparation, Thermal Properties and Thermal Reliability of Palmitic Acid/Expanded Graphite Composite as Form-stable PCM for Thermal Energy Storage *Solar Energy Materials & Solar Cells* 93 2009: pp. 571–576.
<https://doi.org/10.1016/j.solmat.2008.11.057>
21. **Yang, X.J., Yuan, Y.P., Zhang, N., Cao, X.L., Liu, C.** Preparation and Properties of Myristic-palmitic-stearic Acid/Expanded Graphite Composites as Phase Change Materials for Energy Storage *Solar Energy* 99 2014: pp. 259–266.
<https://doi.org/10.1016/j.solener.2013.11.021>
22. **Li, B.X., Liu, T.X., Hu, L.Y., Wang, Y.F., Nie, S.B.** Facile Preparation and Adjustable Thermal Property of Stearic Acid Egraphene Oxide Composite as Shape-stabilized Phase Change Material *Chemical Engineering Journal* 215 2013: pp. 819–26.
<https://doi.org/10.1016/j.cej.2012.11.077>
23. **Chen, Z., Shan, F., Cao, L., Fang, G.Y.** Synthesis and Thermal Properties of Shape-Stabilized Lauric Acid/Activated Carbon Composites as Phase Change Materials for Thermal Energy Storage *Solar Energy Materials & Solar Cells* 102 (7) 2012: pp. 131–136.
<https://doi.org/10.1016/j.solmat.2012.03.013>
24. **Fang, G.Y., Li, H., Liu, X.** Preparation and Properties of Lauric Acid/Silicon Dioxide Composites as Form-Stable Phase Change Materials for Thermal Energy Storage Materials *Chemistry & Physics* 122 (2) 2010: pp. 533–536.
<https://doi.org/10.1016/j.matchemphys.2010.03.042>
25. **Fang, G.Y., Li, H., Liu, X.** Preparation and Properties of Lauric Acid/Silicon Dioxide Composites as Form-Stable Phase Change Materials for Thermal Energy Storage Materials *Chemistry & Physics* 122 (2) 2010: pp. 533–536.
<https://doi.org/10.1016/j.matchemphys.2010.03.042>
26. **Tang, F., Cao, L., Fang, G.Y.** Preparation and Thermal Properties of Stearic Acid/Titanium Dioxide Composites as Shape-Stabilized Phase Change Materials for Building Thermal Energy Storage *Energy and Buildings* 80 2014: pp. 352–357.
<https://doi.org/10.1016/j.enbuild.2014.05.030>
27. **Cao, L., Tang, F., Fang, G.Y.** Synthesis and Characterization of Microencapsulated Paraffin with Titanium Dioxide Shell as Shape-stabilized Thermal Energy Storage Materials in Buildings *Energy and Buildings* 72 2014: pp. 31–37.
<https://doi.org/10.1016/j.enbuild.2013.12.028>
28. **Qian, T., Li, J.H., Min, X., Guan, W.M., Deng, Y., Ning, L.** Enhanced Thermal Conductivity of PEG/diatomite Shape-stabilized Phase Change Materials with Ag Nanoparticles for Thermal Energy Storage *Journal of Materials Chemistry A* 3 2015: pp. 8526–8536.
<https://doi.org/10.1039/x0xx00000x>



© Wang et al. 2021 Open Access This article is distributed under the terms of the Creative Commons Attribution 4.0 International License (<http://creativecommons.org/licenses/by/4.0/>), which permits unrestricted use, distribution, and reproduction in any medium, provided you give appropriate credit to the original author(s) and the source, provide a link to the Creative Commons license, and indicate if changes were made.